UNIVERSITY OF ST. ANDREWS

School of Biology

Structure-Function Studies of the Quinone Binding Site of Cytochrome bo_3 - Ubiquinol Oxidase

M.Phil. Thesis

Ricardo Hugo Jorge Pires

July, 2000

I dedicate this manuscript to the loving memory of my father,
Fernando Ferreira Pires.

CERTIFICATE

I, *Ricardo Hugo Jorge Pires*, hereby certify that this thesis, which is approximately 10 000 words in length, has been written by me, that it is a record of the work carried out by me and that it has not been submitted in any previous application for a higher degree.

Date 1/6/00

Signature of the candidate

DECLARATION

I was admitted as a research student in October 1998 and as a candidate for a degree of M. Phil. in October 1999. The higher study for which this is a record of was carried out in the University of St. Andrews between 1998 and 1999.

Date 1/6/00

Signature of the candidate

CERTIFICATE

I hereby certify that the candidate has fulfilled the conditions of the Resolution and Regulations appropriate for the degree of M. Phil. in the University of St. Andrews and that the candidate is qualified to submit this thesis in application for that degree.

Date ..1...../..6.../..2005.....

Signature of the supervisor..

Acknowledgements

I would like to thank my supervisor, Dr. William John Ingledew for his help, friendship and invaluable scientific stimulus throughout this year.

I would not be able to write this thesis if it was not for all the love and support from my family, namely my mother and sister.

I greatly acknowledge the help of several people within the University of St. Andrews: Dr. Grahm Smith and Dr. Nigel Poolton in the Physics and Astronomy department, for their help with W-Band EPR experiments; Dr. Rona Ramsay for her scientific feedback; and to Irene Tinto and Dr. D. Hunter for their technical support.

I would also like to thank the Minshull Travel Award comity for financing a two-week course on molecular modelling, at the European Molecular Biology Laboratory (Heidelberg, Germany).

A word of thanks is also due to all the friends I've encountered in St. Andrews, and who made my time here so enjoyable.

Last but not least, I would like to thank the Portuguese Scientific Council (*Fundação para a Ciência e Tecnologia*) for funding this work under the grant reference number PRAXIS XXI / BM / 15402 / 98.

1.
Summary

1. Summary

page

2.

List of Abbreviations and Symbols

2. List of Abbreviations and Symbols

$\beta \Rightarrow$ Bohr Magneton

$\nu \Rightarrow$ Frequency

AMPSO $\Rightarrow$ (3-[(1,1-Dimethyl-2-hydroxyethyl)amino]-2-hydroxy-propanesulfonic acid

ATP $\Rightarrow$ Adenosine Triphosphate

Cyt. $\Rightarrow$ Cytochrome

DNase $\Rightarrow$ Deoxyribonuclease

DTT $\Rightarrow$ Dithiothreitol

ETP $\Rightarrow$ Electron Transfer Particles

g $\Rightarrow$ Electron g-value

h $\Rightarrow$ Plank's constant (6.6262×10^{-34} J.s)

EDTA $\Rightarrow$ Ethylene Diamine Tetra-Acetic acid

EPR $\Rightarrow$ Electron Paramagnetic Resonance

ESR $\Rightarrow$ Electron Spin Resonance

Q $\Rightarrow$ Quinone

Q*- $\Rightarrow$ Semiquinone Anion

$QH_2 \Rightarrow$ Quinol

Q-site $\Rightarrow$ Quinone/Quinol binding site

3.

Abstract

3. Abstract

Cytochrome bo_3 – quinol oxidase is a terminal oxidase of the electron transfer chain of *Escherichia coli*. It is responsible for the reduction of dioxygen to water via the donation of electrons from quinones with the concomitant translocation of protons that leads to energy conservation. The work here reported has been conducted in order to characterise the quinone binding site in this complex.

By electron paramagnetic resonance analysis of oriented multilayer samples, it has been possible to establish a preliminary orientation of the semiquinone ring inside the quinone-binding site relatively to the membrane. Data shows that the Y-axis forms a 20^{o} angle with the membrane plane and that X-axis is at 75^{o} to the membrane.

We have also been successful in introducing and stabilising different quinones inside the quinone-binding site (Q-site). This data could suggest that the putative second Q-site (that stabilises semiquinones) is not as tight as initially proposed or does not exist at all rending only one site in dynamic contact with the quinone pool. Furthermore, a different kind of quinone analogue (anthraquinone) with a distinct semiquinone radical signal was observed for the first time. These are important results that could open the possibility to new range of inhibitors, since no studies on 3 aromatic-ring compounds have been done in this system.

EPR analysis of water exchanged deuterated samples confirmed similar previous experiments and indicated that a nearby protonable group is located within the quinone-binding pocket and very near the semiquinone radical.

High field (W-Band) EPR analyses were also conducted in order to isolate the g-anisotropic values of the semiquinone signal. The experiments were not conclusive, but gave good support for current interpretations and indications for future experiments.

4.
Introduction

4. Introduction

4.1. Energy Transduction in *Escherichia coli.*

Energy transduction in aerobically grown *Escherichia coli* is based (like many other organisms) on the electron transport and proton translocation across the cytoplasmic membrane. It is now generally accepted that the major function of membrane-bound redox systems is to translocate protons to the bulk exterior aqueous phase and thus conserve the free energy released by the constituent redox reactions as an electrochemical potential difference of H^+ ($\Delta\mu H^+$; kJ/mol) or protonmotive force (Δp, mV). The cytoplasmic membrane also contains an ATPase/ATPsynthase complex that similarly conserves the free energy released by the hydrolysis or synthesis of ATP according to the difference of proton concentration on the two sides of the membrane. Given this, a highly selective membrane to protons and hydroxide ions is therefore vital to the establishment of a difference of electrochemical potential. The combination of these three main elements (a proton-translocating redox system, a proton translocating ATPase/ATP synthase complex and a membrane highly selectively permeable to ions) results in a delocalized protonmotive force that drives the synthesis of ATP, and other membrane energy dependent functions.

The view described earlier on the mechanism by which cells obtain part of their energy, is known as the chemiosmotic hypothesis (Mitchell, 1976). Several observations agree with this hypothesis:

(a) Protonophores (chemicals that allow the free passage of protons across biological membranes) dissipate the protonmotive force and hence uncouple respiration from ATP synthesis.

(b) ATP can be synthesised at the expense of an artificially generated protonmotive force in membrane vesicles where redox system is absent, but where the ATP synthase complex is present.

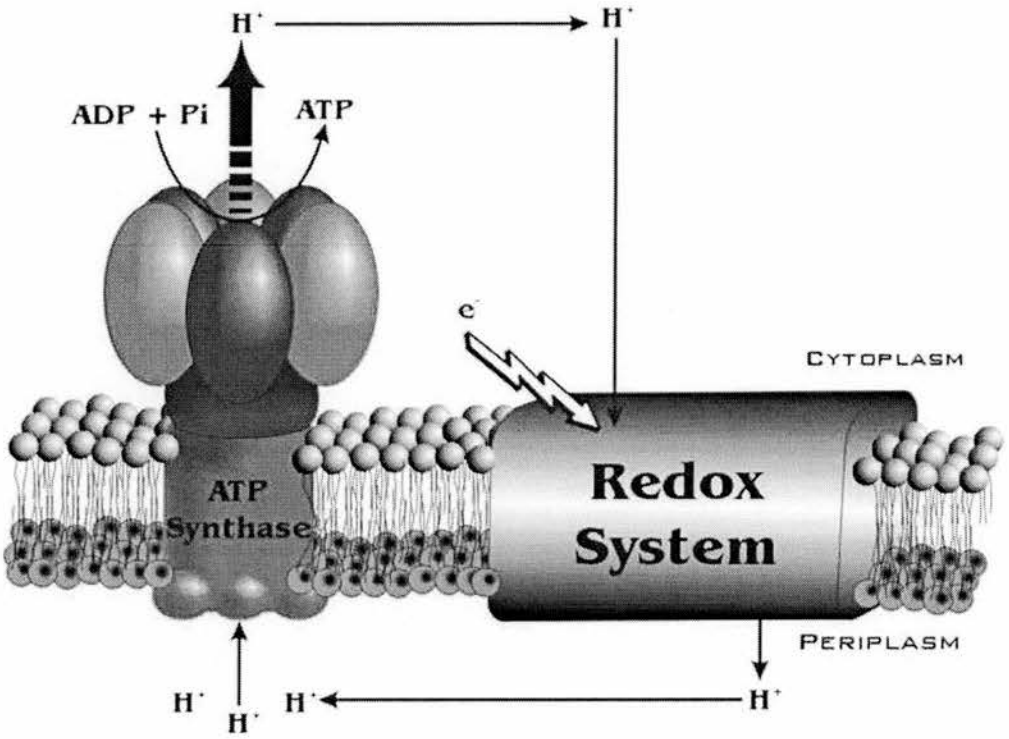

Figure 1. Overall scheme illustrating the chemiosmotic theory.

It is important to note, however, that that this theory is by no means universally accepted (Williams, 1961; Herweijer *et al.*, 1985). Doubts regarding the concept of delocalised protonmotive force as described by chemiosmotic mechanism have been raised after observations that demonstrates:

(a) The absence of a unique relationship *in vitro* between the rate of electron transfer.

(b) The ability *in vivo* of alkaliphiles and halophiles to synthesise ATP when protonmotive force is apparently either very low or absent.

4.2. The Haem-Copper Oxidase Superfamily

During the past several years, it has been recognised that most bacterial oxidases, despite their differences in substrate (Quinol *versus* Cytochrome. *c*), metal content, haem types and affinities to oxygen, are structurally closely related members of one single group called the haem-copper oxidase superfamily. This family also includes their eukaryotic counterparts, which in turn includes the most studied protein of this family: bovine cytochrome *c* oxidase.

Unlike mammalian haem-copper oxidases that may be constituted of up to 13 subunits, bacterial members of this group contain only 3 or 4. Nontheless, they present very similar functional properties, namely, in their proton pumping and oxygen reducing activities.

Subunits I and II of these complexes are the most studied. Subunit I is the most conserved subunit, for example, this subunit of cytochrome bo_3 has 40% sequence similarity with its bovine counterpart cytochrome aa_3 - cytochrome *c* oxidase. The distribution of the haem content throughout this polypeptide seems to be somewhat loose. Haems A, B and O may appear at the oxygen reduction site, while haems A and B occur more often at the low-spin haem region. Nonetheless haem O at this location can also be synthesised rendering a fully active cytochrome oa_3. Therefore, the functional importance of each haem in relation to their location as not yet been reported (Garcia-Horsman *et al.*, 1994). Because of their involvement in oxygen reduction, these complexes are situated at the end of the electron transfer chain (see fig 2).

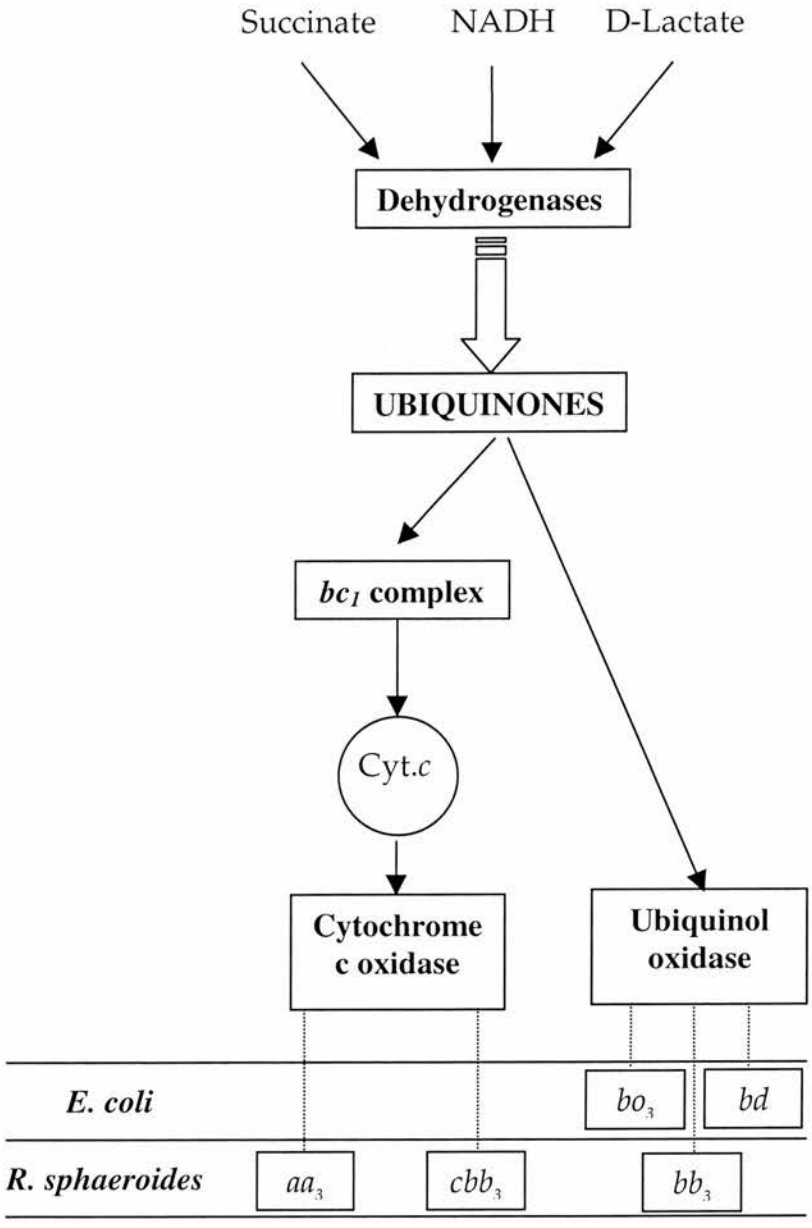

Figure 2: Schematic diagram of a typically branched respiratory chain. Examples of the terminal oxidases of *E. coli* and *R. sphaeroides* are given.

This chain contains several types of dehydrogenases that accept reducing equivalents from different substrates. It also contains a quinol/quinone membrane pool and a bc_1 complex if we are analysing cytochrome *c* dependent respiratory chain.

Depending on the cellular needs and/or environmental pressure, certain bacteria are able to express both branches of the respiratory pathways, thus allowing a better adaptation to energetic requirements.

4.3. Cytochrome *bo*$_3$.- Ubiquinol Oxidase

4.3.1 Genetics & Subunit Composition

The cytochrome *bo*$_3$ ubiquinol oxidase is a member of the haem-copper oxidase superfamily (Garcia-Horsman *et al.*, 1994). This terminal oxidase of the electron transfer chain is commonly found in *Escherichia coli* (*E. coli*), when grown at high oxygen partial pressure (Kita *et al.*, 1984). Cytochrome *bo*$_3$ is therefore involved in the reduction of dioxygen (O_2) to water, as well as in the translocation of protons from the cytoplasm to the periplasm. This is accomplished by a series of one-electron transfer steps where cytochrome *bo*$_3$ acts as an intermediate acceptor of electrons donated by ubiquinol-8 molecules (Kita *et al.*, 1984). Cytochrome *bo*$_3$ has a high degree of homology (in terms of structure) to its mammalian counterpart: cytochrome *aa3* - cytochrome oxidase (fig. 3). However, this homology is not shared with the other terminal oxidase that *E. coli* expresses when grown at low oxygen tension: cytochrome *bd* (Poole and Ingledew, 1987), which has a high affinity to dioxygen and is unable to pump protons across the membrane, having no homology to any other member of haem-copper superfamily (Trumpower and Gennis, 1994).

Cytochrome *bo*$_3$, is an integral membrane protein consisting of one copy each of four subunits, I (74.4 kDa), II (33.1 kDa), III (22.6 kDa), IV (12.0 kDa), encoded by the cyoABCDE operon (Ma *et al.*, 1997). The genes encode

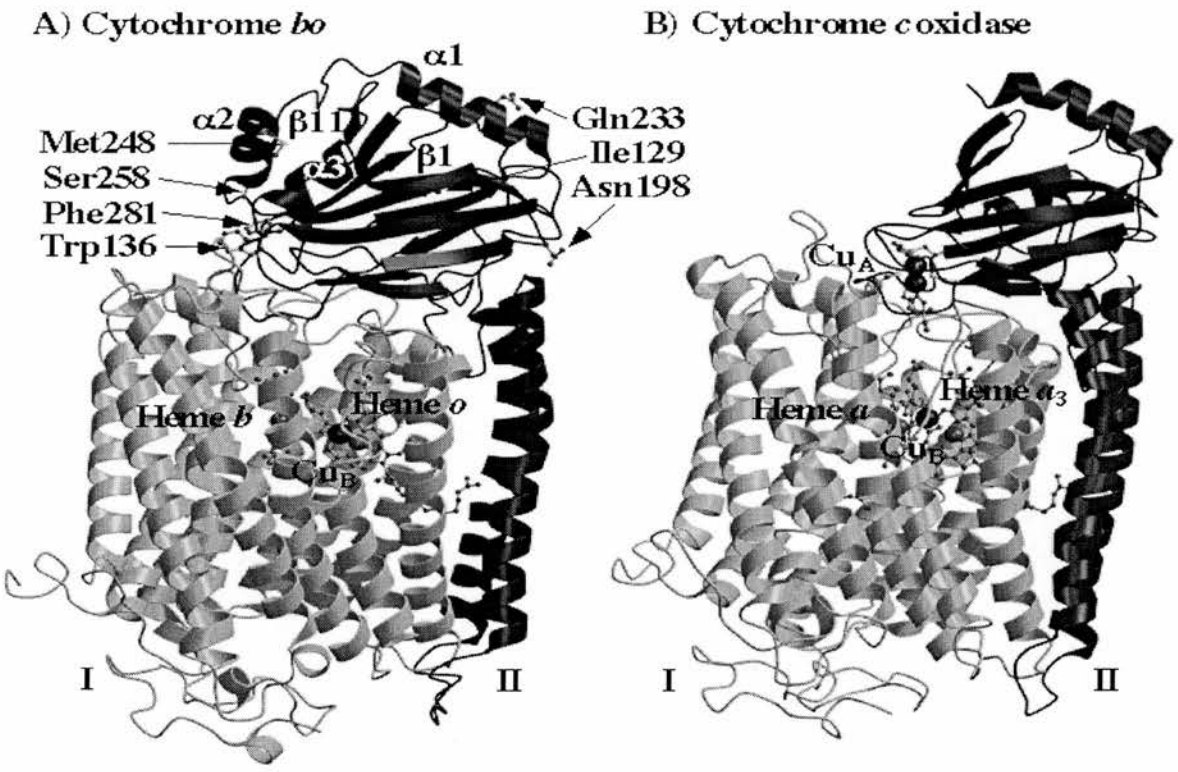

Figure 3: Three-dimensional structure of subunits I and II of both cytochrome bo_3 (model) of *E. coli* and cytochrome *c* oxidase (X-ray structure) of *Paracoccus denetrificans*. Residues that were mutated in studies of quinone-binding / electron-transfer are indicated in cytochrome bo_3 (taken from Sato-Watanabe *et al.*, 1998).

subunits II (cyoA), I (cyoB), III (cyoC), IV (cyoD). CyoE encodes for protohaem IX farnesyltransferase required for the biosynthesis of haem *o* (Saiki *et al.*, 1993). Studies on the *aa3*-type cytochrome *c* oxidase isolated from *Paracoccus denitrificans* (*P. denetrificans*) have clearly demonstrated that subunits I and II are sufficient both for cytochrome *c* oxidase activity and for coupling the electron transfer reactions to proton pumping across the membrane (Hendler *et al.*, 1991). Subunit I is highly conserved within this superfamily and contains both a low spin, six-coordinate haem component and a haem-copper binuclear centre, which is the site where oxygen is reduced to water (Babcock and Wikstrom, 1992; Saraste, 1990). In *E. coli* bo_3-type oxidase, haem b_{562} occupies the low-spin site, whereas haem *o* is the high spin

haem associated with a copper atom called CuB (Ma *et al.*, 1993), thus forming a binuclear center (fig.4).

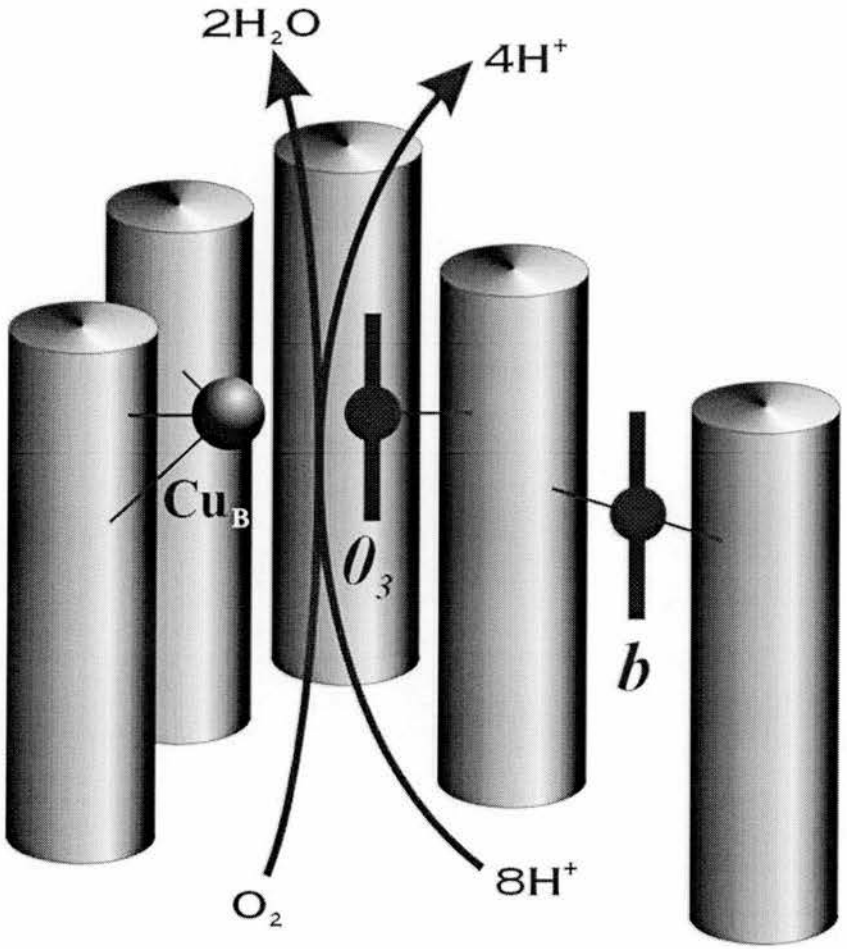

Figure 4: A three-dimensional scheme of the binuclear centre and haem b_{562} in subunit I. Each compound involved in the redox reaction is shown in stoicheometreic amounts (exception is made for the four electrons). Taken and adapted from Svensson and Brzezinski, 1995.

For those members of the oxidase superfamily that utilise cytochrome *c* as a substrate, subunit II plays a clear function. Subunit II is implicated in the binding of cytochrome *c* and, in addition, it contains a second copper moiety (CuA) that is directly involved in the oxidation of ferrocytochrome *c* (Saraste, 1990). For quinol oxidases (like Cytochrome bo_3) however, there is no copper atom and quinol molecules are the ones oxidised, instead of cytochrome *c*. The gene encoding this subunit reveal 34.9 kDa polypeptide, but studies by Gennis

and co-workers (Ma *et al.*, 1997) have demonstrated that this polypeptide suffers a post-translational modification. This subunit is initially synthesised with a N-terminal signal sequence that is proteolytically processed to form the mature subunit II, which is a lipoprotein with covalently attached lipids at the new N-terminus, which is localised at Cys25 (Ma *et al.*, 1997). However, site directed mutagenesis experiments that block the processing reveal that this lipid group is not essential to produce a fully functional quinol oxidase (Ma *et al.*, 1997). It is in subunit II that the quinone binding site is localised (for more information on quinone binding sites, see the following sections).

As it was said previously, subunits III and IV seem to have no important role from the catalytic point of view of cytochrome bo_3, hence the lack of information on these two subunits. However some studies have been carried out in order to probe the function of subunit IV. This subunit is conserved in bacterial haem-copper terminal oxidases (Chepuri *et al.*, 1990). It has been shown that 75% removal of subunit IV by proteolytic digestion did not affect proton pumping activity of caa_3-type cytochrome *c* oxidase from thermophilic *Bacillus* PS3 (Prochaska *et al.*, 1996). This is consistent with previous observations that the two-subunit preparations of the *E. coli* ubiquinol oxidase (Kita *et al.*, 1984) and of cytochrome *c* oxidase from *P. denetrificans* (Ludwig and Schatz, 1980; Hendler *et al.*, 1991) have been reported to be fully functional; therefore, subunit IV is dispensable for the catalytic function of the bacterial haem-copper terminal oxidases.

In contrast, Papa and colleagues (Villani *et al.*, 1995; Papa *et al.*, 1994) found that a deletion in the *Bacillus subtillis* (*B. subtilllis*) of the *qoxD* gene encoding subunit IV of *aa3*-type menaquinol oxidase, significantly depressed respiration and proton pumping, but did not affect the content of the *aa3*-type cytochrome

in the membranes. Thus, they concluded that subunit IV is essential for the function of *aa3*-type menaquinol oxidase in *B. subtillis*. Studies carried out by Anraku and co-workers (Saiki *et al.*, 1996) have revealed that two-thirds of the polypeptide chain at the C-terminal region is required for the functional expression of the enzyme, and that subunit IV assists the CuB binding to the binuclear centre in subunit I during biosynthesis or assembly of the oxidase complex.

4.3.2 Kinetics of Electron Transfer & Proton Pumping

Due to the fact that the possibility of two Q-sites is not completely established, the kinetics of electron and proton transfer in cytochrome bo_3 will be discussed taking into account the possibility of one Q-site. This option was taken due to the structural similarities of ubiquinol and cytochrome c oxidase complexes that have been reported, and that could indicate a same underlying mechanism. Therefore, for sake of clarity, only the possibility of one Q-site shall be explored into more detail from a mechanistic point of view.

Electrons from ubiquinol (UQH2) which binds to subunit II, are first transferred to haem b_{562} and then to the binuclear centre, where dioxygen is bound and reduced to water [for a review, see Babcock and Wikstrom (1992) and Ferguson-Miller and Babcock (1996)].

One of the techniques commonly used to investigate the reaction between O_2 and the reduced enzyme is the flow-flash technique [developed by Gibson and Greenwood (1963)]; the fully reduced enzyme with carbon monoxide (CO) bound to haem *o* is mixed with an O_2 containing solution.

Oxidation of the enzyme is slow (10^{-1} s^{-1}) because the reaction is limited by the CO-off rate. Immediately after mixing, CO is photodissociated and reaction between the fully reduced enzyme and O_2 is studied using various spectroscopic techniques. Several studies have been made applying this method to study the electron transfer reactions in cytochrome *bo*$_3$ (Svensson and Nilsson, 1993; Orii *et al.*, 1995; Puustinen *et al.*, 1996; Svensson *et al.*, 1995, 1996) and to the proton uptake and release in cytochrome *bo*$_3$ (Hallen *et al.*, 1993; Svensson *et al.*, 1995, 1996) and in cytochrome *aa3* (Hallen and Nilsson, 1992).

Work carried out using flow-flash technique in combination with spectroscopic methods (Svensson and Brzezinski, 1997) lead to the proposal of this mechanism (fig. 5). The data suggested that redox reaction would go through three phases.

The first one, with the oxidation of haems *b* and *o* and formation the peroxy intermediate; the second and third electron-transfers were only observed with enzyme containing bound quinol, and are there fore attributed to electron-transfer reactions associated with quinol oxidation (Puustinen *et al.*, 1996).

The first phase is similar in both cytochrome *bo*$_3$ and in bovine cytochrome *c* oxidase (Svensson and Brzezinski, 1997), indicating that binding of O_2 to the binuclear centre, with the formation of a peroxy intermediate, would be the initial step.

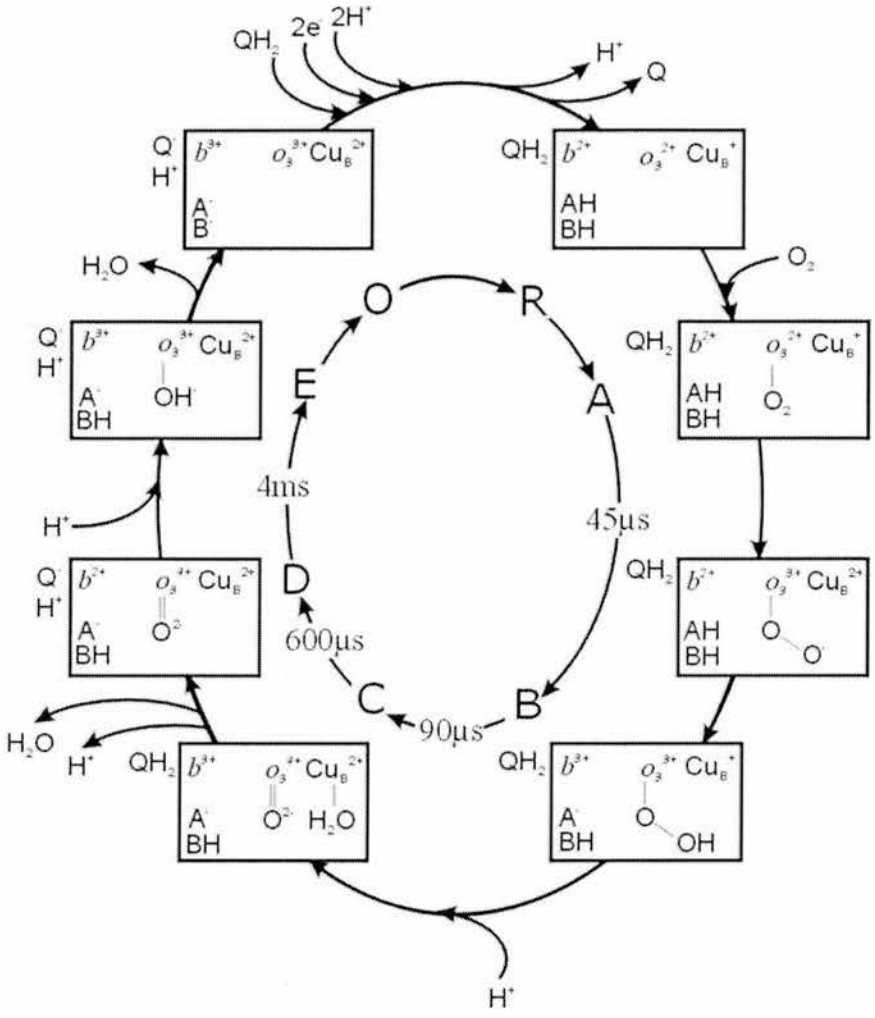

Figure 5: Proposed mechanism for redox reaction that leads to dioxygen reduction and quinol oxidation in cytochrome bo_3. See text for more details.Taken from Svensson and Brzezinski, 1997.

In the following phase, because it could only be observed with bound ubiquinol and due to the increase of the absorbance at 430 nm the authors suggested that in this step an electron from the bound quinol, would be transferred to the haem *b562*, with a time constant of ~700 µs, followed by electron transfer from haem *b562* to the binuclear centre with a time constant of ~4ms.

According to Svensson and co-workers (1997), since the electron-transfer time constants (in both cytochrome *o* and in bovine cytochrome *c*

oxidase) are smaller (45 μs and 80 μs respectively) than proton uptake (90 μs in the two cases), they thus conclude that the former is controlled by the later.

4.4. Quinol, Quinones and Semiquinones.

Several books and reviews have been written that discuss the importance of quinones from a biological point of view, and these can be found in literature already mentioned. A book is also available where a chemical approach is done (Morton, 1965).

Quinones and quinols (also designated as hydroquinones) are membrane bound mobile carriers of reducing equivalents between quinone reducing proteins and quinol oxidising proteins. They normally comprise substituted *p*-benzoquinones and naphthoquinones. The former ones are synthesised in the form of ubiquinone (found in aerobically grown bacteria) while naphthoquinones appear in chloroplasts in the form of plastoquinones and menadione (found in anaerobicaly grown bacteria).

Quinones undergo a $2H^+/2e^-$ reduction via a semiquinone anion observable by EPR. This characteristic allows us to study these proteins during turnover. Most free biological semiquinones are highly unstable with stability constant at pH 7.0 of 1×10^{-10} (Michell, 1976). Therefore, they can only be observed at the site of stabilisation of the free radical.

4.5. Quinone Binding Sites

4.5.1 Overview

Quinone/Quinol binding sites are found in quinone-dependent respiratory and photosynthetic complexes. In addition to their importance in catalysis in electron transfer systems involved in energy transduction, these loci are the site of action of numerous inhibitors, including pesticides, herbicides and antibiotics. Quinone/Quinol binding sites are therefore of significant economic and industrial importance. Despite their ubiquity and importance, studies on a number of quinone/quinol sites (including the structure of the photosystem II reaction centre) have not yet resolved structural motifs defining these sites.

Quinone/quinol binding sites (Q-sites) can either be: Acceptor sites (oxidises quinol - fig. 6); Donor sites (Reduces quinone) or Pair Splitting sites. In the first two cases the electrons are transferred to the same acceptor, whereas in the third case the electrons are directed to two substrate molecules that are differently located in space, having different thermodynamic properties.

However, in all three Q-sites we observe that the electron transfer reaction is achieved by two one-electron-transfer steps, therefore forming a free radical intermediate, which gives rise to EPR signals. Due to the very low stability of biological semiquinones, full redox reaction can only occur if this free radical is stabilised.

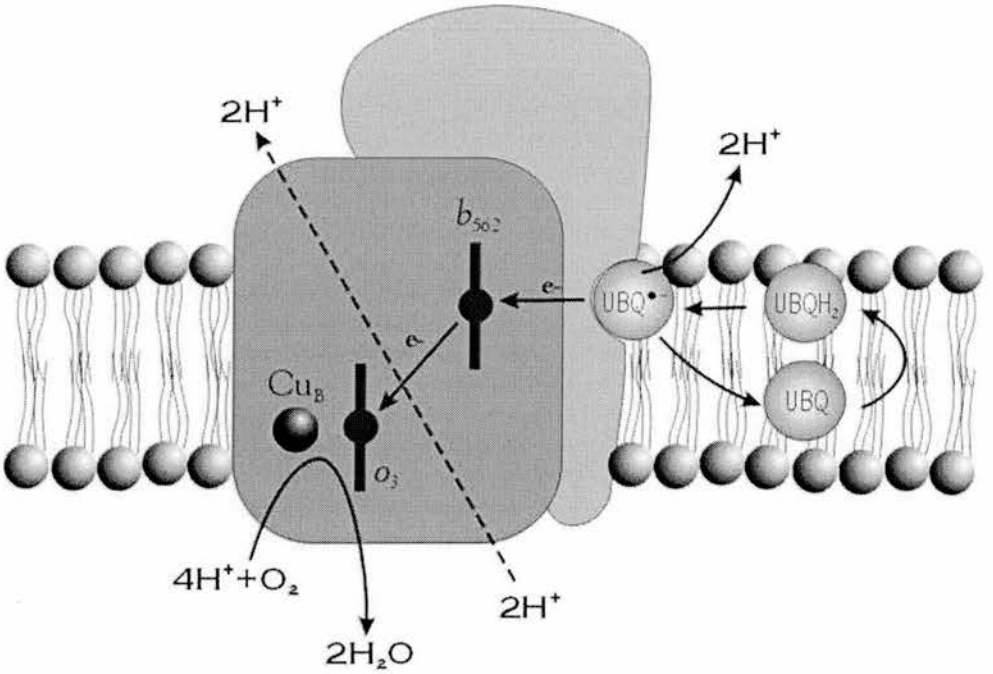

Figure 6: Scheme of the possible mechanism for dioxygen reduction and quinol oxidation. This model takes into account the existence of only one Q-site, in analogy to what happens in cytochrome *c* oxidase and according to published data (Ingledew *et al.*, 1995)

4.5.2 Subunit II of Cytochrome *bo*$_3$ Ubiquinol Oxidase

The ability to stabilise the semiquinone is one of the most important features of donor/acceptor Q-sites. Quinone/quinol binding proteins often have two Q-sites in order to facilitate coupling of one-electron redox chemistry to an two-electron acceptor/donor (Kotlyar *et al.,* 1990; Warncke *et al.,* 1994). Typically, one of these binding sites is primarily responsible for stabilising the semiquinone radical, whereas the other acts as the electron input/output site (Musser *et al.,* 1997). Based in part on this fact, Musser and co-workers (1993) suggested that the cytochrome *bo*$_3$ complex has two Q-sites.

Subsequently Sato-Watanabe and colleagues (1994) reported a tightly bound quinone-8 molecule, in the isolated cytochrome *bo*$_3$, that could not be

removed with high concentrations of ubiquinol-1 or inhibitors. These investigators therefore concluded that another high affinity Q-site (Q_H) could exist that would trap the semiquinone free radical during enzyme turnover. In the above paper, it is suggested that the low affinity Q-site (Q_L) would be the binding site for ubiquinol. The second high affinity Q-site (Q_H) is proposed to be close to, both the Q_L and the haem b_{562}.

A semiquinone EPR signal was reported (Ingledew *et al.*, 1995) which appears to be a single species but which exhibits unusual hyperfine structure. This data was previously interpreted by Sato-Watanabe and colleagues (1994) as an indication of interaction between the semiquinone and haem b_{562}, however this is unlikely as at the potentials at which the semiquinone signal is maximal, the haem b_{562} is almost completely reduced. Ingledew *et al.*, suggests that the hyperfine signal is more likely due to interaction with protons.

On the other hand, there is little agreement in terms of the role of this second Q-site between those that postulate its existence. Sato-Watanabe and co-workers (1994) defend that the strongly bound semiquinone at the novel Q-site (Q_H) mediates the electron transfer from ubiquinol to haem b_{562}. Furthermore, it is said that the bound ubiquinone would be in dynamic equilibrium with the quinone/quinol pool.

Musser's group (Musser *et al.*, 1997) says that the first reported quinol oxidation site (denoted Q_A) acts as a pair-splitting site, where one of the electrons is transferred directly to the haem *o* and the other to the haem b_{562}. This electron is then transferred to the new second Q-site (denoted Q_B) allowing the reduction of ubiquinone to quinol. According to Musser (1997),

the raman and UV/IR spectroscopy data previously reported (Sato-Watanabe *et al.,* 1994) support this theory.

4.6. Principles of EPR Technique.

Electron Paramagnetic Resonance (EPR) - also designated Electron Spin Resonance (ESR) - is a spectroscopic technique that takes advantage of differences in the population of unpaired electrons, to probe their surrounding environment. Several books and review papers on the subject are available (Hoff, 1989; Atherton , 1994).

For simplicity, let us consider a paramagnetic substance that contains a free unpaired electron (S = 1/2). In the absence of magnetic field, all spins are oriented randomly at the same energy level. When this paramagnetic sample is placed in a magnetic field (H), the magnetic moment of unpaired spins will tend to be aligned either anti-parallel or parallel to the direction of the magnetic field - this is called, Zeeman splitting. Therefore, spins in the sample are divided into two populations having different energies: $-1/2g\beta H$ for anti-parallel spins and $1/2g\beta H$ for parallel spins; where g is a constant value called electron g-value and β the Bohr Magneton constant. In EPR we observe a resonance transition between these two induced spin populations. The energy difference (ΔE) between these two spin states is dependent on the strength of the applied field (H). When microwave with an energy $h\nu$ (h is the Plank's constant and ν the microwave frequency) is applied to the system, and H is scanned, a transition takes place when ΔE between the two states ($g\beta H$) becomes equal to $h\nu$.

EPR spectra are generally obtained by scanning the magnetic field to find the resonance position with a fixed microwave frequency. Different terminology is applied to the EPR apparatus based on this factor (e.g. X-Band EPR relates to 9 GHz spectrometers, while W-Band EPR are related to machines operating in the 90 GHz region).

Because EPR is not a very sensitive technique, spectra are not recorded as an absorption signal, but rather as first derivative of the former one. Modulation of the magnetic field frequency and phase sensitive detection, are used to increase the signal to noise ratio.

However, an unpaired electron within a paramagnetic species often does not have only one resonance position (g-value) to the magnetic field. This is due to the 3D delocalization of the electron within its orbital. Metal clusters, and semiquinones are examples of such systems. In these cases, we do not talk about one g-value, but rather we speak of up to three g-tensors (g_x, g_y, g_z). Each of these values, correspond to the parallel orientation of the magnetic field to one of the axis of the electron orbital. If an electron tends to have several different specific positions within its orbital (like in *p* and *d* orbitals, rather than being scattered (like in *s* orbitals), it will give rise to different signals, as they are parallel to the magnetic field. Isotropy is therefore related with measurements that are independent of the orientation, whereas anisotropic signals are due to one same electron delocalized in the space in a specific way. The only two symetries that reflect this anisotropy are designated as axial - when the delocalization is observed mainly in a plane: $g_x \cong g_y < g_z$ and rhombic - for a delocalization in a set of three orbitals each perpendicular to the other two: $g_x \neq g_y \neq g_z$. In the case of some free radicals (e.g. semiflavins and semiquinones), all three g-tensors, may be very close to each other, giving rise

to an EPR signal where is very difficult to observe each g-tensor independently. In systems like these, it is often necessary to do computer simulation or run experiments at higher fields. In the case of complex systems like proteins, computer simulations can be very difficult since other factors (such as hyperfine splittings due to neighbouring nuclei within the protein matrix) can be involved. This is often the reason why, it is necessary to recur to EPR at higher magnetic field frequency, so that interferences can be minimised and hence the g-tensors properly observed.

The g-tensors are an important way to study the structure of a paramagnetic centre in an oriented sample. If we take into consideration a sample that is oriented on the plane of the magnetic field, as the former one is turned the direction of the magnetic momentum of the electron eventually will meet the absolute direction of the magnetic field. When the direction of the field is parallel to the spin of the electron, the transition will take place at the lowest intensity (i.e. at the highest g-value).

A problem that occurs when analysis is conducted at high magnetic field (H), is that energy separating the parallel and anti-parallel spin states becomes quite large ($\Delta E = h\nu = g\beta H$). This yields, according to the Boltzman distribution equation (see bellow), a small ratio between these two states, thus giving rise to small signals since only a few electrons actually are involved in the transition.

Boltzman Distribution Equation

$$\frac{Np}{Nap} = e^{\left(-\Delta E/kT\right)}$$

Where: *Np*, is the number of electrons in a parallel spin; *Nap*, the number of electrons with an anti-parallel spin; ΔE, is the energy difference between the two states; *kT*, is the average thermal energy that is characterises each system.

When, the electron population tends to stay in only one of the states, we designate the system as saturated, due to a quantum process known as spin-lattice relaxation. The rate at which this phenomenon: occurs is known as spin-lattice relaxation time (T_1). This process is easily seen at very low temperatures and in systems where the paramagnetic unit is not very coupled to the surrounding matrix. Due to the magnetic field applied the electrons tend to stay in energised spin state. However in order to produce a visible EPR signal the spins need to relax to a lower energy state so that they can be excited again and thus maintain equilibrium between the two energy levels. Saturation arises when due to the very low temperatures used, the vibrational energies of the atoms in the system becomes so small, that the paramagnetic unit does not interact with the matrix. This leads the spins to stay in the upper energy level, not relaxing back because they are unable to interact with the surrounding lattice and therefore loose their energy. In less coupled systems analyses have to be conducted at higher temperatures, to make up for the poor interaction.

On the other hand, if the temperature, at which we run the experiment is too high, another kind of relaxation will take place. The phenomenon under analysis is called spin-spin relaxation and the parameter under consideration, is the time at which this process occurs (T_2). High temperatures give to much energy to a system, this means that vibrational energies rise in a way that Heisenberg's uncertainty principle has to be taken into account. Due to the atomic movement in the sample, it becomes impossible to determine a precise

spins transition energy. The Heisenberg's uncertainty principle reflects itself in the EPR signal line-shape in the form of line broadening. The spins in the upper state due to dipolar interactions relax quickly but they exchange their position with a spin in a lower energy level, thus shortening the time of a spin in the upper state without having effect on the population ratio. *In extremis*, this could result in signal disappearance.

But relaxation rates are not the only parameters affecting the line-shape of a spectrum. Another aspect to analyse, and that is highly connected to the atomic environment of the paramagnetic centre, is the hyperfine splitting pattern. Hyperfine interactions occur between the magnetic momentum of the unpaired electron, and the magnetic momentum of a spinning nucleus, that reinforces or reduces locally the applied magnetic field. Therefore, depending on the number of nuclei and the magnetic characteristics of each nucleus the splitting pattern will reflect this structural arrangement. If we consider an unpaired electron orbiting around a carbon atom, with a covalent bond to one hydrogen atom, the proton, because it can have two different spin values, will give rise to the splitting of the signal into two signals with the same intensity. As said before, this pattern will change depending on the interacting nucleus and the number these same nuclei.

After this short explanation it is easily seen, that EPR is quite a powerful technique to study these systems in a dynamic manner. The purpose of this project is therefore to bring new insights in to the dynamic ability of the Q-site of cytochrome bo_3 to exchange and stabilise different quinones and acquire structural information for how the endogenous ubiquinone sits in the quinone pocket.

2.

Material & Methods

5. Material & Methods

5.1. Bacterial Strain

The *Escherichia coli* (*E. coli*) strain GO105/pJRHisA was used throughout the work. This strain (a gift from Prof. Robert Gennis, University Urbana-Campaign, USA) overexpresses, five fold, cytochrome bo_3 with a 6 histidine tag at the carboxyl *terminus* of subunit II. This transformed strain also contains the gene for resistance to ampicillin and is unable to express the other terminal quinol oxidase - cytochrome *bd*.

5.2. Media and Growth Conditions

5.2.1. Inoculum Preparation

Single colonies of GO105 taken from LB agar plates containing 100 μg/mL of ampicillin, were inoculated in 100 mL of Luria Broth supplemented with 50 μg/mL of ampicillin. After overnight growth in a 37 °C room with high agitation, this culture was used to prepare 1L of inoculum with the same media, and grown at 37 °C for 8 h.

5.2.2. Fermentor Operating Conditions and Media

The 1 L culture was used to innoculate a 10 L working volume fermentor (MicroFerm® Fermentors, New Brunswick Scientific, NJ, USA). Cells were grown in a media containing per litre: 4.5g, KH_2PO_4; 1.5g, K_2HPO_4; 2.4 g, tryptone; 2.4 g, yeast extract; 6.0 g, casamino-acids; 1.2 g, $(NH4)_2SO_4$; 12.0 mL, glycerol; 1.2 mL, trace elements solution; 0.1 mL, 10 mg/mL $CuSO_4$; 0.1 mL, 5 mg/mL $FeCl_2$. The pH was adjusted to 7.2.

Immediately prior to inoculation, 0.6 g of ampicillin, 0.6 g of nicotinic acid and 0.6 g of thiamine were added to the media, via a sterilising filter. Cells were then grown at high rate of agitation and in a highly aerated media at 37 ^oC until mid-logarithmic phase (this minimises the release of proteases that could cleave the histidine tag).

5.2.3. Trace Elements Solution

This solution consisted of: 3 mM $FeCl_3$; 2 mM MnCl; 1.2 mM $CoSO_4$; 4.5 mM boric acid; 15 mM $ZnCl_2$. The pH was adjusted to 7.0.

5.3. Harvesting Fermentor Cell Cultures

Cells where harvested by filtering the media using a cross-flow membrane system (Millipore, UK). The retentate, was then centrifuged at 10,000×g for 15 min in a Sorvall® RC-5B Superspeed Centrifuge (Dupont, USA). The cell pellet was then washed twice with 5 mM Tris-HCl, pH 7.8 and finally

resuspended in this same solution and kept in "pea form" by freezing drops of the cell suspension in liquid nitrogen. The cells where stored this way at -20 °C until required.

5.4. Preparation of Electron Transfer Particles

Frozen cells (70 to 100 g, wet weight) where thawed and resuspended to 150 mL in 5 mM Tris/HCl, pH 7.8 with 2 mg DNase (Type I), 10 mM Benzamidine and 10 μL of 0.5 M $MgCl_2$. The suspension was passed twice through a French press (American Instrument Company, Silver Spring, USA) at $1.0x10^8$ Pa. Large cell debris and unbroken whole cells were separated from the membranes by centrifugation at 10,000×g for 15 min. The pellet was discarded and the supernatant centrifuged at 150,000xg for 1h in a Beckman® L8-55M Ultracentrifuge (Palo Alto, California, USA) at 4 °C. The sedimented membranes where then resuspended with the help of a hand homogeniser in 5 mM Tris/HCl, pH 8.0 and kept in "pea form" until required.

5.5. Purification of Cytochrome *bo*$_3$ - Quinol Oxidase

Membrane fragments where resuspended in 50 mM K_2HPO_4, pH8 with 1.25% *n*-Octyl-β-D-glucopyranoside and 1% Triton X-100 to promote the extraction of cytochrome *bo*$_3$. The mixture homogenised with a hand homogeniser was left stirring for 1 h in an ice-bath.

Insoluble material was then removed by centrifugation at 100,000×g in a Beckman® L8-55M Ultracentrifuge (Palo Alto, California, USA) for 45 min at 4 °C. The supernatant was collected and when a red/pink pellet remained, this was resuspended in 50 mM K_2HPO_4, pH8 and kept at -80 °C for another extraction round.

The soluble protein was precipitated by saturating the solution up to 70% with ammonium sulphate with the help of a mortar and a pestle while keeping the mixture stirred in an ice-bath. A protein pellet was obtained by centrifuging the mixture at 150,000×g for 1 h. The precipitate was then resuspended in 50 mM K_2HPO_4, pH8 with 0.05% N-Lauroylsarcosine and 1mM EDTA and dialysed against 2L of this same buffer, overnight at 4°C.

All the insoluble material was removed by centrifuging at 100,000×g for 45 min and the oxidase complex present in the supernatant was concentrated up to 50 μM.

The concentration of cytochrome bo_3 was monitored spectrophotometrically. The difference spectrum between dithionite reduced and oxidised protein was used to calculate the its concentration by analysing the 560nm region peak (fig. 9) using an extinction coefficient of 20.5 mM^{-1} cm^{-1} (Mitchell *et al.*, 1995).

5.6. Oriented Membrane Multilayers

5.6.1. Sample Preparation

Electron Transfer Particles (ETP) were thawed and washed twice in 5 mM TES, pH 8 with 0.1 mM EDTA, by homogenising the suspension and centrifuging it at 150,000×g for 1h at 4°C in a Beckman® L8-55M Ultracentrifuge (Palo Alto, California, USA).

Meanwhile, dialysis membrane sheets where soaked in 10 mM EDTA for 15 min to avoid possible metal interference in the EPR analysis. These sheets where then partially dried and a thin layer of 1% colloidon in 70% Ethyl/Ether was spread on one of the sides of the membrane and left to evaporate. The membranes with the colloidon layer facing up were then fitted between an pollycarbonate hemispherical base and a hollow cylinder made from the same material and introduced inside centrifuge tubes. The membrane suspension was loaded inside the polycarbonate cylinder and the whole apparatus was centrifuged at 50,000×g for 90min in a swing-bucket rotor at 4 °C.

After centrifugation the ETP multilayers associated with the dialysis membrane where dried under a steady and gentle stream of nitrogen, after which they where cut with a scalpel into 2-3mm wide strips, inserted into EPR tubes and kept in liquid nitrogen until required.

5.6.2. EPR Analysis Settings

The oriented multilayers were incubated in 50 mM AMPSO, pH9 with 60% Glycerol, 2mM decylubiquinone and 3mM Dithiothreitol (DTT) for 45 min at room temperature. EPR analysis were conducted at 100K in a ER 200D

electron paramagnetic spectrometer (Bruker Analytische Messtechnik MBH, Germany) equipped with a ESP3220 Data System (Bruker Analytische Messtechnik MBH, Germany) running with a ESP300e software system (Bruker Analytische Messtechnik MBH, Germany). Modulation frequency was set to 100 kHz and the amplitude to 1.0 G. The conversion time used was 81.92 msec and the time constant was 327.68 msec. The receiver gain parameter was $2x10^4$. The frequency used was 9.44 GHz and the microwave power was 2 mW. Spectra reflect the accumulation of 10 scans.

5.7. Quinone Analogues EPR Studies

5.7.1. Deuterium Oxide Exchanged Samples

Cytochrome bo_3 extracted as described in section 2.5 was loaded into a microdialysis apparatus, and dialysed against a D_2O solution containing 50 mM AMPSO, pD8.6; 0.05% N-Lauroylsarcosine and 1 mM EDTA. The pD was adjusted by titration with minute size grains of solid KOH and taking into account the following relation described by Glasnoe and Long, 1960.

$$\mathbf{pH_{electrode} = pD + 0.4}$$

To achieve a 98% replacement of water with deuterium oxide, the dialysis was conducted with equal volumes of sample and buffer, and in an isocratic 6 steps fashion, with each step lasting for 1h. The relationship of volume of D_2O buffer to volume of sample was 1.

Efficiency of water replacement by D_2O was judged by EPR analysis with added decylubiquinone, taking into account spectral differences as reported by Hastings, 1997.

5.7.2. Quinone-Analogues Used

The following quinone-analogues were used: Decylubiquinone; 2,3-dichloro-5,6-dicyano-1,4-benzo-quinone; Anthraquinone and Duroquinone (tetramethylquinone). All these reagents were of analytical grade and are available commercially.

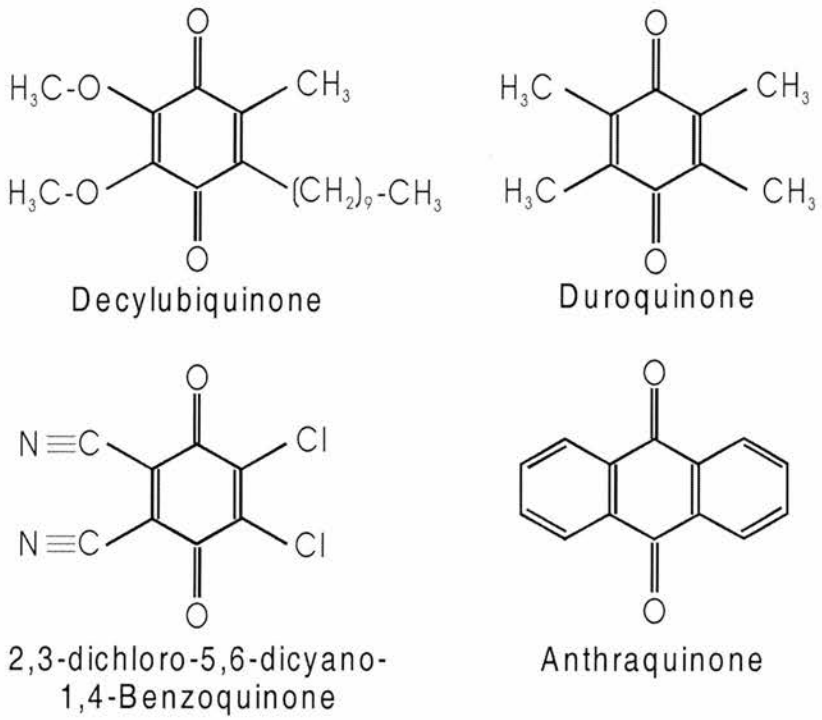

Figure 8: Structural formulas of the quinone-analogues used.

5.7.3. Sample Preparation and X-Band EPR Analysis

Cytochrome *bo*$_3$ complex (either with or without D_2O replacement) was loaded into an EPR tube with 2 mM of Quinone-Analogue and 1 mM DTT. A series of control experiments were also conducted, where cytochrome *bo*$_3$

samples were titrated with DTT in concentrations ranging from 0.3 mM up to 2.3 mM. All samples were incubated at room temperature for 45 min and then frozen in liquid nitrogen until required.

EPR analysis was conducted at 100 K, in a ER 200D electron paramagnetic spectrometer (Bruker Analytische Messtechnik MBH, Germany) equipped with a ESP3220 Data System (Bruker Analytische Messtechnik MBH, Germany) running with a ESP300e software (Bruker Analytische Messtechnik MBH, Germany). Modulation frequency was set to 100 kHz and the amplitude to 1.0 G. The conversion time used was 81.92 msec and the time constant was 327.68 msec. The receiver gain parameter was $2x10^4$. The frequency applied was 9.44 GHz, the microwave power was 2 mw and 20 scans were accumulated for each spectrum.

5.7.4. W-Band EPR Analysis

Samples used in the X-band analysis were used in the 90 GHz scan. Samples were loaded into a capillary EPR tube via a micro-syringe, and immediately frozen in liquid nitrogen. Analysis were conducted in a 90GHz spectrometer equipped with an Oxford Instruments RT magnet with a continuos flow cryostat (3-300K). Detailed parameters for each analysis are depicted below each spectrum, in the following sections.

6.

Results & Discussion

6. Results & Discussion

6.1. UV/Vis Spectral Analysis

The spectra in fig. 9, show that cytochrome bo_3 was correctly extracted from the membrane fragments. The absorption pattern is the same as those that have been published so far (Puustinen *et al.*, 1992). The data suggest that the results here reported are related to an apparently native conformation of the whole molecule.

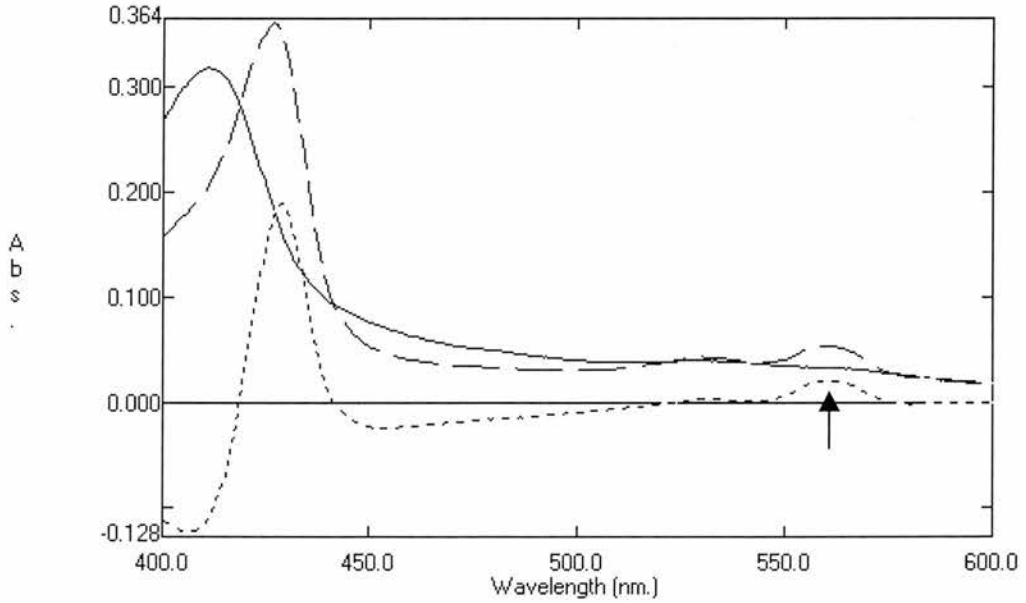

Figure 9: UV/Vis spectrum of cytochrome bo_3 oxidised (solid), reduced (dashed) and the difference spectrum of reduced minus oxidised spectra (doted). The arrow indicates the absorption peak used to quantify the cytochrome bo_3 content.

Several reports have been published regarding mixed-haem occupancy in proteins of overexpressing E. coli strains (Puustinnen and Wikström, 1991), rending in this case, a cytochrome oo_3 instead of the normal cytochrome bo_3. Haems B and O differ in position 2 of the porphyrin ring where vinyl group is

replaced by a long hydrophobic hydroxyethylfarnesyl side chain in haem O. Despite this variation in the structure of one of the prosthetic groups, the enzymatic activity and polypeptide composition of the enzyme remain virtually the same (Puustinnen *et al.*, 1992).

6.2. Oriented Multilayers

The results obtained in the oriented multilayers experiments show that the quinone ring tends to have a fixed orientation within the quinone pocket. Although results indicate that these sites tend to be quite promiscuous in terms of binding capacity to other quinone analogues, a definite orientation is apparent and seen when the sample is rotated relatively to the magnetic field. Not clearly shown in fig. 10, these changes are easily seen in the difference

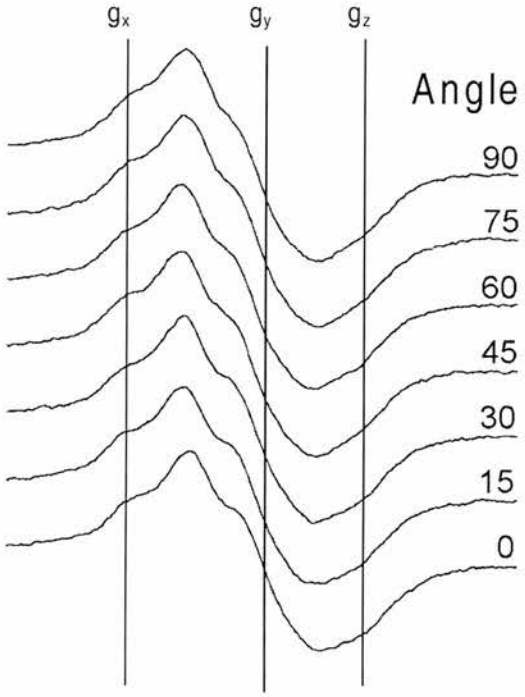

Figure 10: EPR spectra of oriented membranes with different angles of orientation to the magnetic field. Approximate areas for measurement of each g-tensor are shown. Spectra are centred at g=2.00 and where obtained as outlined in section 5.6

spectra in fig. 11. The variation of the centred g-value between each analysed angle is approximately 1G. Affected by certain instability in the microwave frequency being applied and due to the small variations observed it is impossible indicate the orientation of the quinone ring to the membrane plane without some degree of error.

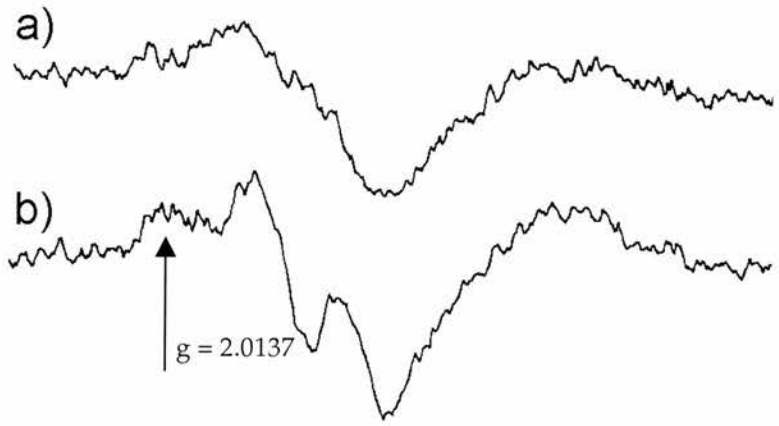

Figure 11: Difference spectra of oriented multilayers with distinct angles: a) 90° minus 0°; b) 45° minus 0°. Spectra centred at g=2.00.

Table 1: g_y-anisotropy values obtained according to each angle. An average g_y is shown as well as the standard deviation (SD) for this value.

Angle	H (Gauss)	g_y	Average g_y	SD
0	3427.557	2.0073	2.0073	0%
15	3426.842	2.0077	2.0074	0.04%
30	3426.842	2.0056	2.0063	0.11%
45	3426.699	2.0057	2.0067	0.15%
60	3426.699	2.0057	2.0059	0.03%
75	3426.842	2.0056	2.0057	0.01%
90	3426.842	2.0056	2.0055	0%
105	3426.556	2.0057		
120	3425.984	2.0061		
135	3426.699	2.0078		
150	3427.843	2.0071		
165	3427.843	2.0071		
180	3427.557	2.0073		

NOTE: Since these values are supposed to be symmetrical from 90°, an average-g_y was calculated having in attention the following consideration:

$$g_y = \{g_y [90\text{-}X\times15] + g_y [90+X\times15]\}\div2$$

Where X is a discrete number between 0 and 6 inclusive and the value obtained in squared brackets is the angle to which we should refer the appropriate g-tensor value in order to calculate the average.

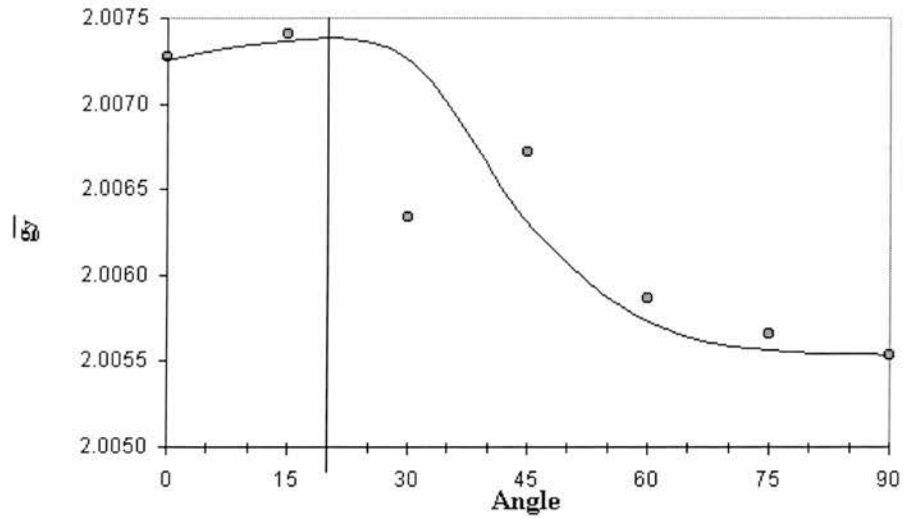

Figure 12: Plot of average g_y for each angle. A hand drawn hypothetical curve is shown as well as the 20° supposed orientation.

Nonetheless, preliminary analysis of the data has been made. The line-shape of the EPR signal is due to both g-tensors and hyperfine splittings that superimpose on each other, giving the spectra obtained. Although both parameters are orientation dependant, we can make an approximation when we assume that the hyperfine interactions are symmetrical in their field position in relation to zero crossing point. Thus, we can say that the only parameter that determines the zero crossing is the g-anisotropy (MacMillan *et al.,* 1997). Given this, a set of measurements was conducted where the dry membrane strip would be in rotated in different angles to the direction of the magnetic field. The field position of the zero crossing was determined by integrating the obtained spectra and locating the point of maximum signal height on the applied field scale.

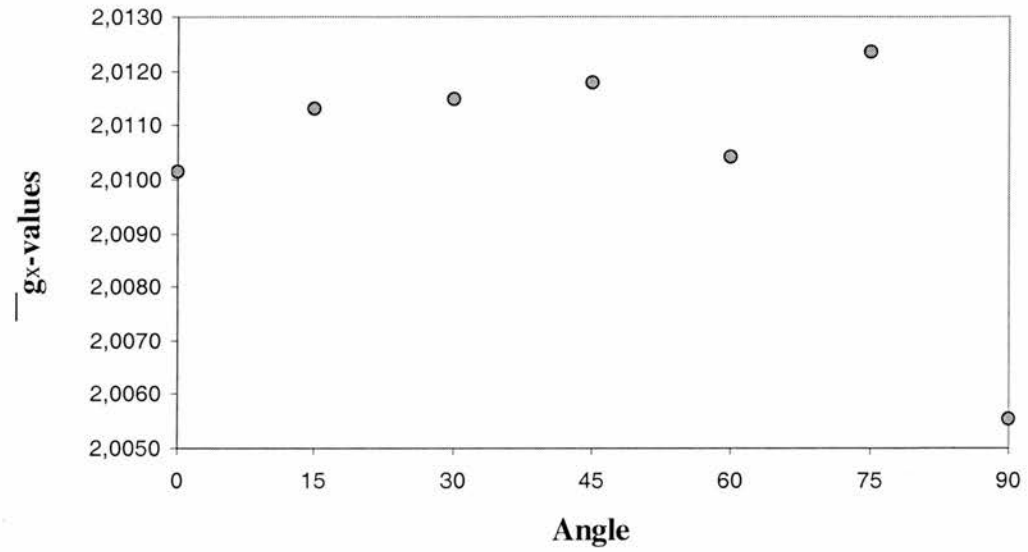

Figure 13: Variation of the average g_x-anysotropy value with angle (see text for more details).

Assuming the Y-axis as a line parallel to the quinone ring and at 90° in the same plane to the line that connects the two oxygens, X-axis (MacMillan *et al.,* 1997) we have calculated that the Y-axis is at approximately 20° of the membrane plane (fig 12 and tab. 1). Similar calculations have been made to determine the angle of the X-axis to this plane (fig. 13) and we estimate that it forms a 75°. However, the supposed g_x-tensor could be much more influenced by oriented hyperfine splittings then the g_y-tensor. The approximation made for the later tensor (g_y) may not be valid for the former one (g_x). This renders a less accurate angle value for the X-axis that needs vital confirmation at high field EPR. From the data obtained here it is impossible at this stage to estimate the angle that the Z-axis forms with the membrane plane. X-Band EPR does not allow the resolutions of g_z tensor given the signal height obtained nor its isolation from hyperfine splittings.

The results divulged here are very similar to the conclusions published by Murray and co-workers (1999) using molecular modelling techniques. A 24° angle of the Y axis to the membrane plane was reported in the cited paper.

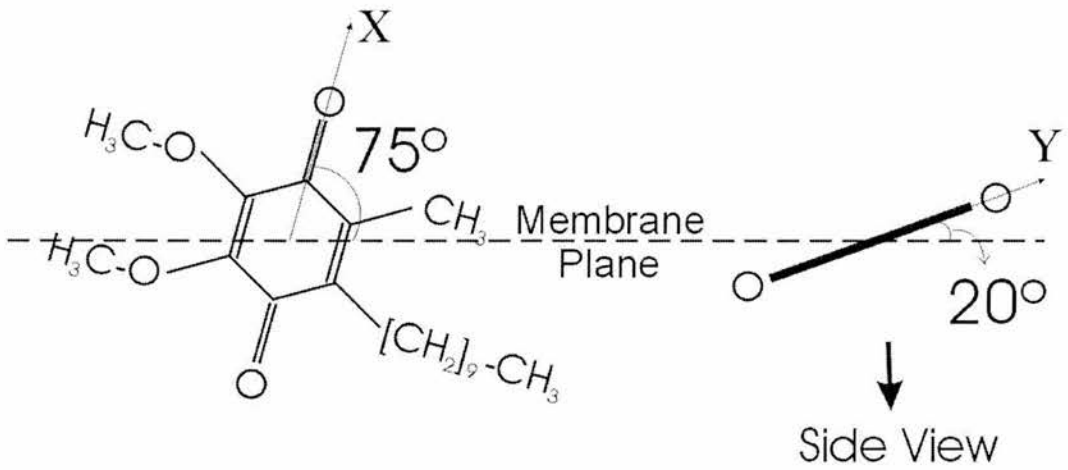

Figure 14: Orientation of the decylubiquinone ring inside the quinone pocket (see text for details).

From the difference spectrum obtained in fig 11, a signal (g = 2.0137) arises from what is believed to be due to a hydrogen atom of a nearby protonable residue (see section 6.3.2. for further explanation). The confirmation as to whether or not this residue is involved in semiquinone stabilisation requires other techniques. Although this signal proves to have clear angular dependence, the rules governing the orientation dependence of this hyperfine splitting are different thus the calculations done to determine the orientation of the quinone ring may not be applicable.

6.3. X-Band EPR - Quinone Analogues Experiments

6.3.1. Control Experiment

An initial control study was conducted in the attempt to certify that once applied the extraction protocol described, and using the same amount of reducing equivalents, there were no endogenous quinones bound to the putative low affinity quinone binding site (Q_L) reported by Sato-Watanabe and co-workers (Sato-Watanabe, M. *et al.*, 1994).

Figure 15, shows the typical spectrum observed in titrated samples, over a wide range of reducing equivalents. No free radical signal was detected which means that results here reported are not due to the influence of loosely bound quinones.

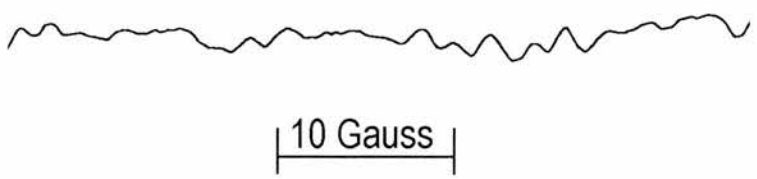

Figure 15: EPR spectrum of cytochrome bo_3 in water reduced with 1mM DTT with no exogenous quinone Analogues being added. The spectrum is centred at g=2.0.

6.3.2. Water substitution by Deuterium Oxide.

In order to provide a better resolution and interpretation of the hyperfine splitting pattern and g-tensors of the semiquinone signal, attempts were made to replace water with deuterium oxide. Exchangeable protons from nearby protonable residues could be involved in the stabilisation of the semiquinone anion. In order to achieve this, a 98% replacement is usually needed.

As it is seen by comparison of figures 16 and 17, the splittings in the D_2O exchanged sample are still quite unresolved. This could be mainly due to the concentration of stabilised free radical within the sample, that is not high enough to produce a signal with a signal good resolution of the g-tensors and hyperfine pattern. protons, due to the smaller magnetic moment of deuterium nuclei (Hales. *et al.*, 1981). In fact this is clearly observed as the line-broadening effect was much reduced when both figures are compared.

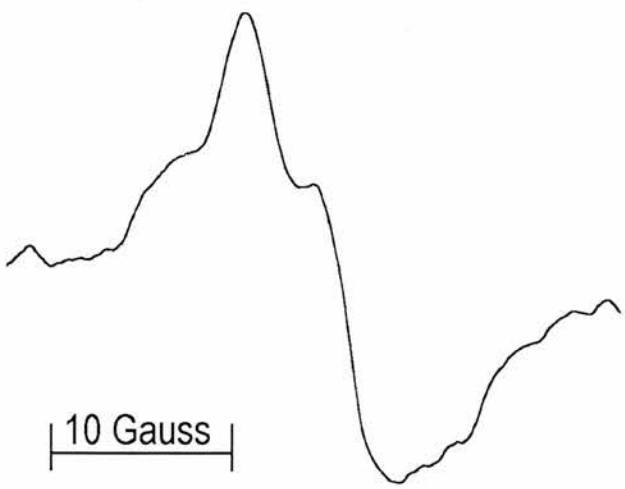

Figure 16: EPR spectrum of cytochrome bo_3 poised with decylubiquinone in D_2O and reduced with 1mM DTT, as described in section 5.7.

Although both g_x tensor values and hyperfine splittings due to non-exchangeable protons are still quite unresolved, this experiment show that water protons give rise to hyperfine splittings, one of these (g = 2.0137) show orientation dependence. It is therefore likely that a residue with a protonable group is located nearby.

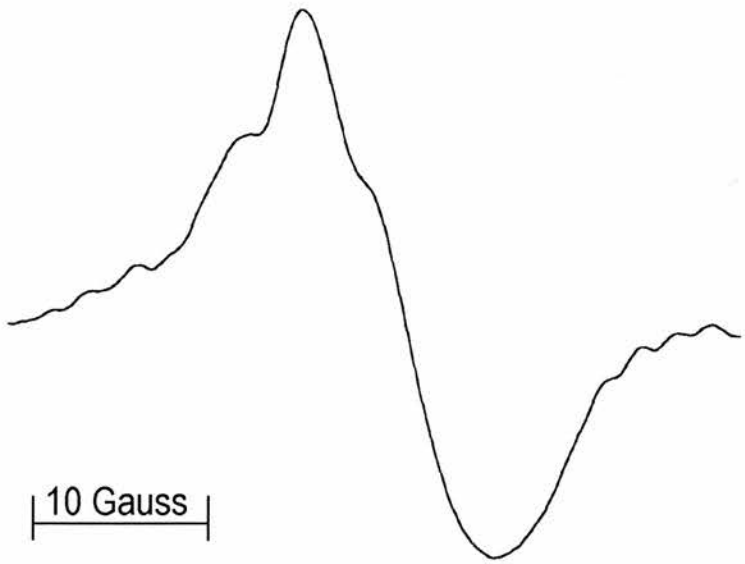

Figure 17: EPR spectrum of cytochrome *bo*$_3$ poised with decylubiquinone in water and reduced with 1mM DTT, as described in section 5.7. This spectrum shows a slight signal broadening which is partially due to the poor quality of background correction as well as the proton's magnetic momentum.

6.3.3. Quinone Analogue Binding Experiments.

As it is possible to see from the comparison of the spectra in figures 16 to 20, a whole range of quinone analogues have been tried and successfully introduced inside the Q-site.

The different spectra indicate that it is possible for the protein to stabilise different semiquinones. The data therefore contradicts the conclusions drawn by Anraku and colleagues (Sato-Watanabe *et al.,* 1995) as for the existence of a second tighter Q-site.

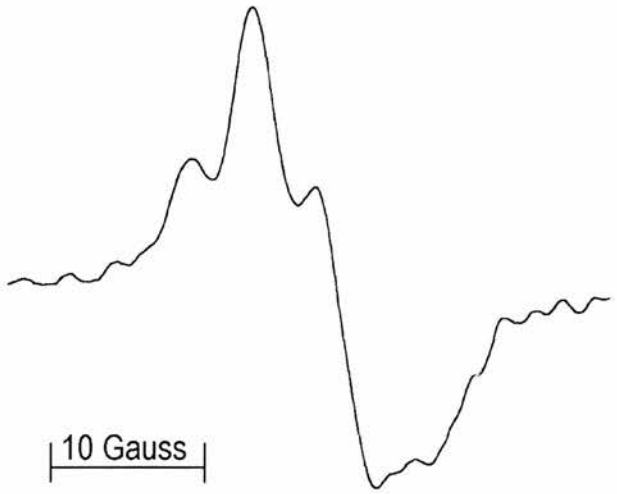

Figure 18: EPR spectrum of cytochrome bo_3 poised with anthraquinone in D_2O and reduced with 1mM DTT, as described in section 5.7.

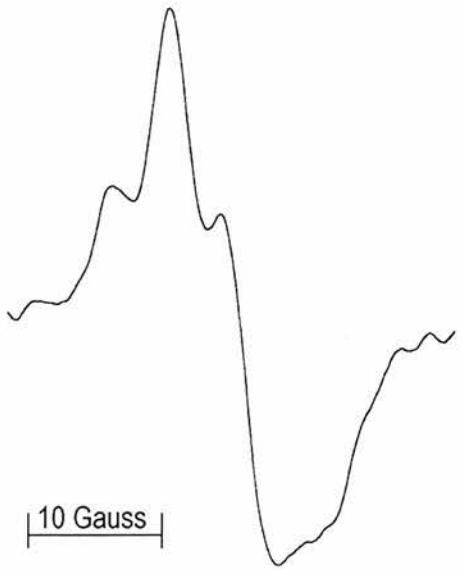

Figure 19: EPR spectrum of cytochrome bo_3 poised with Duroquinone in D_2O and reduced with 1mM DTT, as described in section5.7..

In the cited paper, different cytochrome bo_3 samples reduced in the presence and in the absence of a potent Q-site competitive inhibitor (2,6-dichloro-4-dicyanovinylphenol) had shown no difference in the EPR spectrum obtained. It is possible to see marked differences in the line-shape of the several spectra. Analysis of figures 17 and 18 reveal that the hyperfine pattern became more defined. In conjunction with data published previously (Hastings, 1997) it seems feasible to assume that these patterns could be due to hyperfine interactions of the delocalised unpaired electron with the protons covalently linked to the substituent carbons. They become more marked if more of these

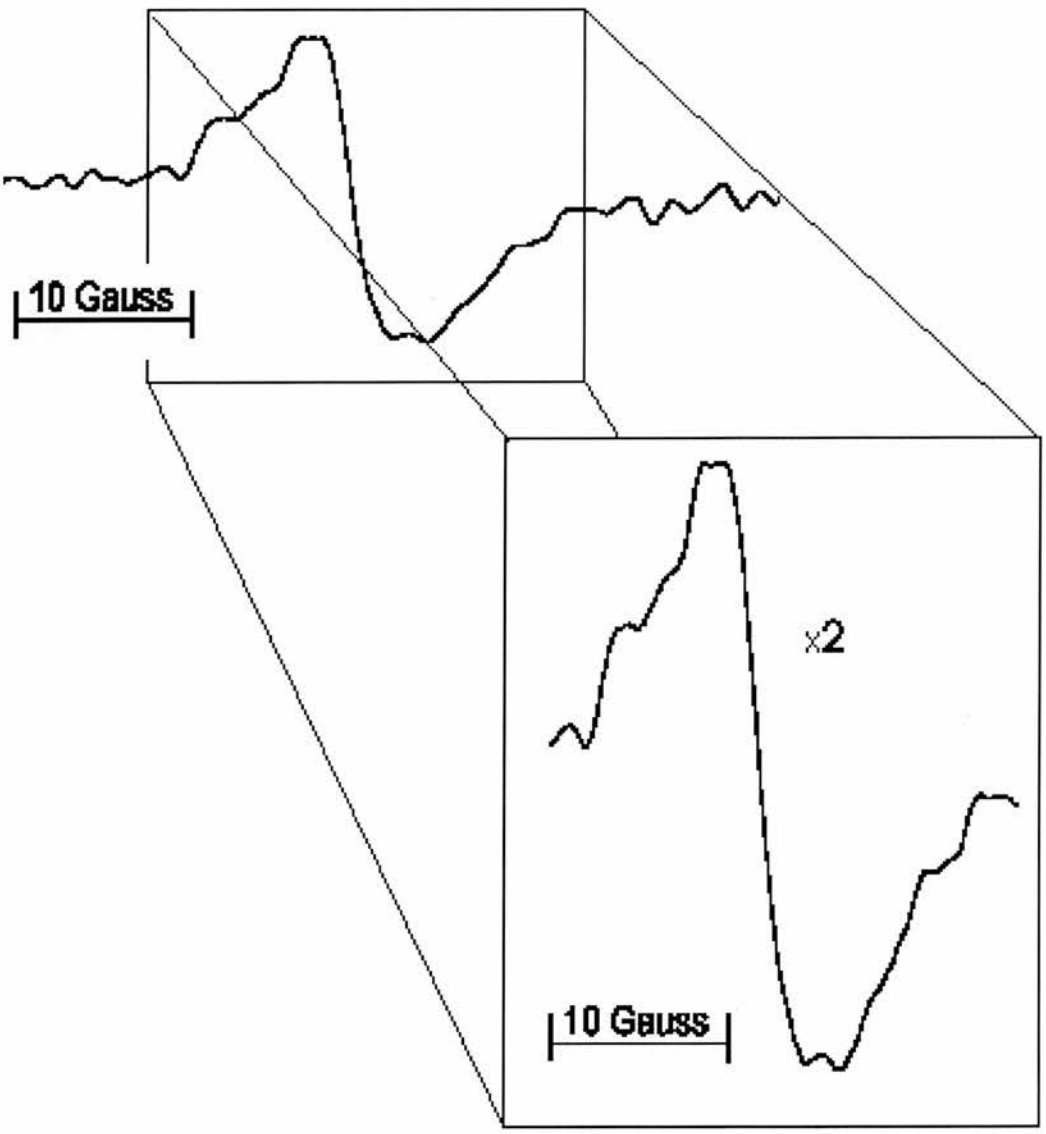

Figure 20: EPR spectrum of cytochrome bo_3 poised with 2,3-dichloro-5,6-dicyano-1,4-benzoquinone in D_2O and reduced with 1mM DTT, as described in section 5.7.

groups exist near the ring. It is interesting to notice how these feature are completely absent in the spectra of 2,3-dichloro-5,6-dicyano-1,4-benzoquinone. Furthermore, new paramagnetic interactions seem to have risen or appeared in fig 20. Since the substituents in this analogue do not cause hyperfine interactions, it seems that the later one could be due to interactions with the protein matrix.

The extraction protocol gives a preparation free of any bound quinones. This conclusion would be later on supported by the group that initially proposed the idea of the second Q-site (Sato-Watanabe *et al.*, 1998). Nonetheless, citing kinetic data, they explain this as due to a conformational change in the protein.

Furthermore, the results divulged in this manuscript show for the first time that it is possible for a quinol binding site to stabilise a flat 3 ring quinone molecule (anthraquinone). This shows how promiscuous these sites can be, and opens the possibility to new range of inhibitors. These new anthraquinone based inhibitors could also prove to be quite specific to certain quinone-binding sites, due to its bulky three ring structure. Until now, only one and two rings based analogues have been tried and successfully stabilised or used as inhibitors in quinone-binding sites.

It seems to be highly unlikely that due to the described purification protocol, the protein could: unfold; release the tightly bound quinone; exchange it by a large inflexible ubiquinone analogue such as anthraquinone; refold again and still be able to stabilise it. Such mechanism could only be possible if the quinone being stabilised would be in dynamic contact with the quinone pool and therefore at the surface of the complex.

6.4. W-Band EPR - Quinone Analogues Studies

In the attempt to resolve the g-anisotropy values, high field EPR was conducted in samples already proven (by X-band) to have a signal. Samples poised with anthraquinone as described in section 5.7.3 were scanned at

90GHz with different amplitude modulations. These experiments revealed an increase in the signal height as expected, and slight broadening of the line. It is clearly seen, that the rise of the free radical signal [see (4) in figure 21] is accompanied by the rise of other small signals with a saturation line-shape [see (1), (2) and at g=2.0075 (not marked) in Figure 21].

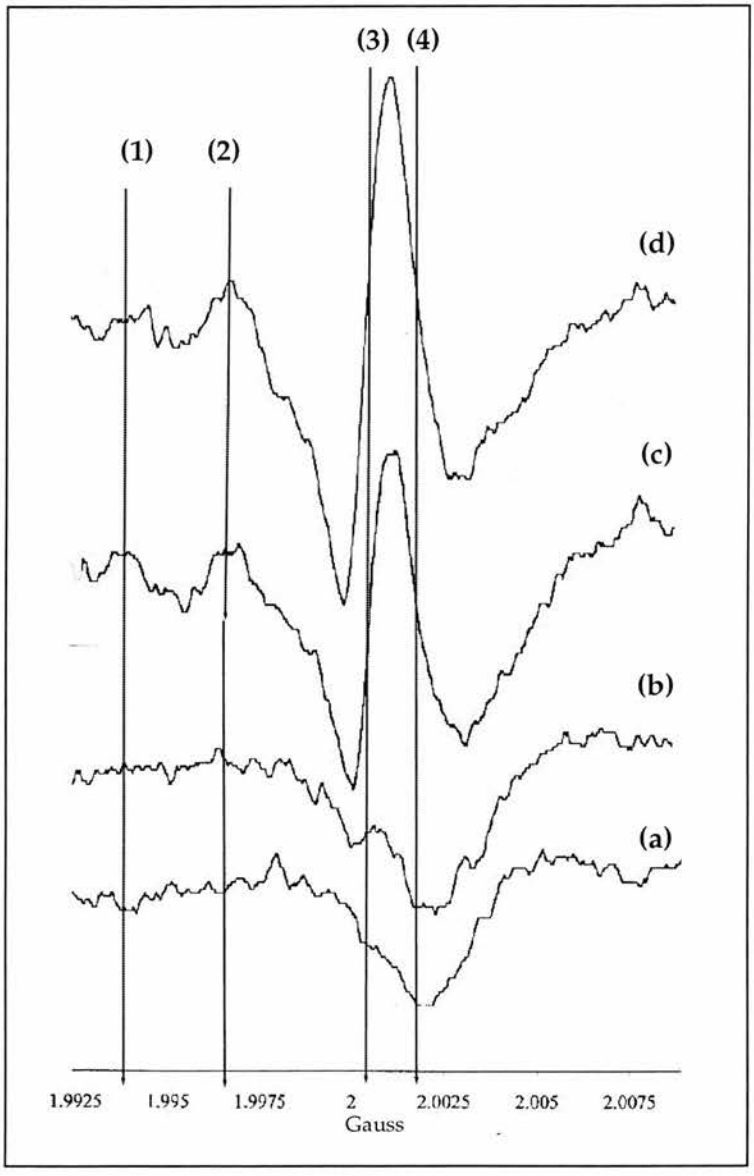

Figure 21: W-Band EPR spectra of semianthraquinone. Different amplitude modulations were conducted in order to get the best signal to noise ratio. All spectra were obtained at 5K; 1.5KHz modulation frequency; scan rate 1.7G/s; time constant 1 s. other parameters were: (a) Modulation Amplitude 0.3G at 92.854 GHz; (b) Modulation Amplitude 1G at 92.854 GHz (c) Modulation Amplitude: 4G at 92.855 GHz (d) Modulation Amplitude 6G at 92.857 GHz.

Since the signal width is around 40G and (while its width is half in X-Band) and accounting the fact that the g-tensors do not move in relation to each other, we should assume that the side signals are therefore either due to protein metal centres, or other contaminant metals.

By comparing figures 22 and 23 we can clearly see the differences between the two. In figure 23 there is a slight broadening of the signal at g=2.0030. Given the parameters used, at 20K the spin-spin relaxation effect for spins in transition metal ions might start occurring causing the broadening of the spectra observed at the mentioned g-value.

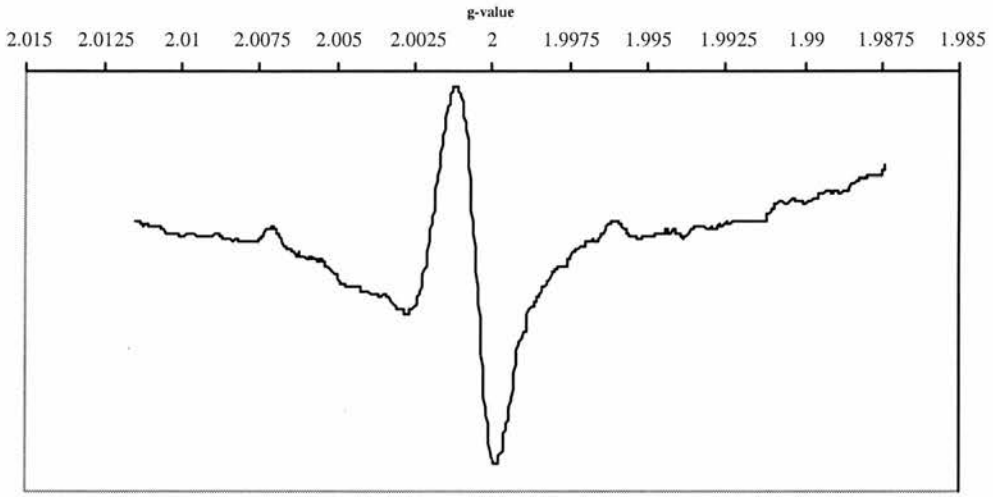

Figure 22: W-Band EPR spectrum of semidecylubiquinone in cytochrome bo_3. Parameters were: Microwave Frequency 92.920 Ghz ; Temperature 5K; Modulation frquency 1.5G; modulation amplitude 6G; Scan rate 1.7 G/s; Time constante 1s; 1 scan.

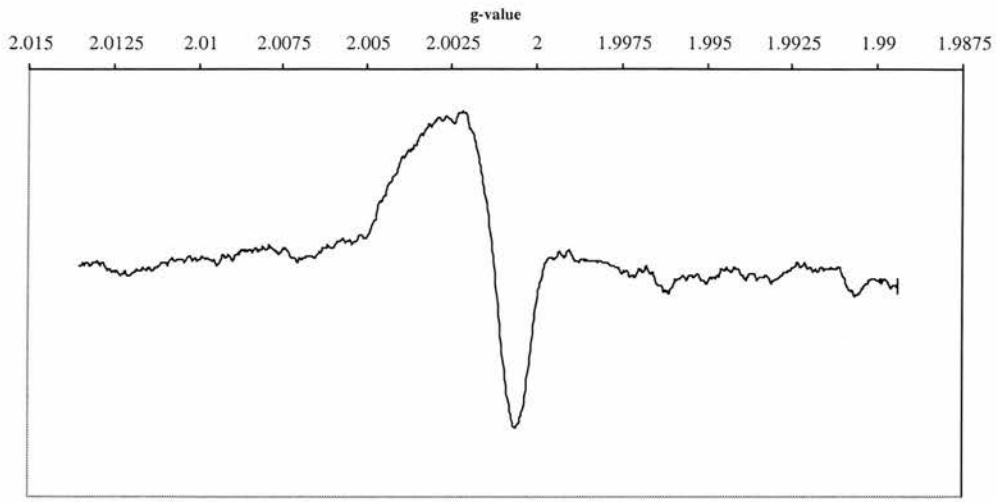

Figure 23: W-Band EPR spectrum of Cytochrome bo3 poised with decylubiquinone in D2O. Parameters were: Microwave Frequency 93.004GHz; Temperature 20K; Modulation Frequency 1.5 KHz; Amplitude Modulation 6G; Scan Rate 0.7G/s; Time Constant 1s; 1 scan.

If we then take a broader view of the spectra (fig. 24), we find out that the spectra obtained so far are the result of underlying transitions that might obscure the semiquinone signal. Since the purification procedure applied

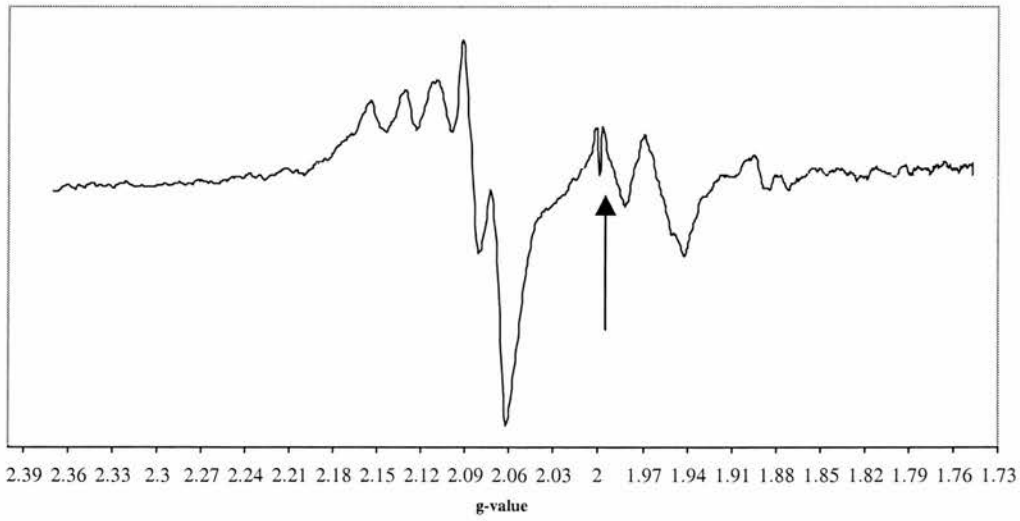

Figure 24: Broader W-Band EPR scan of decylubiquinone poised cytochrome bo_3 sample. Scan was carried out at 16K; Microwave Frequency 92.911GHz; Modulation Amplitude 6G; Modulation Frequency 1.5KHz; Scan rate 1.7G/s; Time Constant 1s; 1 scan. Sample prepared as outlined in sections 5.7.1. and 5.7.4. The arrow indicates the field position where the transition due to the semiquinone occurs. In this spectrum copper splittings from de protein's binuclear centre are also observed between g = 2.17 and g = 2.04

greatly enriches the samples in their ubiquinone oxiadase content but does not render samples free of some protein contaminants, some traces of metallic paramagnetic centres can cause this interference. Iron-sulfur clusters, for example, are known to have transition signals in this region of the spectrum (e.g. 3Fe-4S in the oxidised form and 4Fe-4S in the reduced form). Furthermore, since free radical signals are characterised by having a zero crossing region at g=2.00, that in the case of biological systems does not varies much in shape, it does not seems possible for other free radicals to be involved in the low resolution of the semiquinone signal.

Analysis of figures 22 and 23 reveals that the distance between the upper and lower extremities of the signal has doubled in this experiments compared to spectra obtained in X-band. Since g-tensors do not move in relation to each other, this interference obviously obscures even more the true g-values, and therefore it is impossible given the results to establish all the exact three tensors for the semiquinone radical.

7.

Conclusions

7. Conclusions

From the results reported here we were able to establish a preliminary orientation of the semiquinone within the quinone pocket relatively to the membrane plane. According to our calculations it sits approximately with it's Y-axis at 20° to the membrane plane and the X-axis at 75°. The interference of hyperfine interactions greatly diminished the quality of the data for the measured angle of the X-axis with the membrane plane.

Deuterated samples, confirmed previous experiments that pointed the existence of a protonable group in the Q-site near the semiquinone. This could indicate that water could be part of the mechanism, by which the quinone is stabilised. Other experiments, such as the combination of molecular modelling studies with specific point mutations would be extremely valuable to reach a conclusion.

We were also able to stabilise different quinones within the Q-site, as it is demonstrated by the different spectra. Certain features have disappeared and others emerged in all spectra, which could be the result of the difference of substituents in the quinone analogues and a change in the structural rearrangement of the protein, in order to accommodate and stabilise a different semiquinones inside it. This data contradicts work published by several authors claiming the existence of a second, tighter quinone binding site (Sato-Watanabe *et al.*, 1994; Orii *et al.*, 1995 and Musser *et al.*, 1997). A good partition coefficient of the ubiquinone with the extraction detergent mixture is required for a successful extraction of ubiquinone-free protein. The extraction protocol used, renders a fully functional protein, capable of not only stabilising ubiquinone, but anthraquinone, duroquinone and 2,3-dichloro-5,6-dicyano-1,4-benzoquinone. A tight site as envisioned by Sato-watanabe & Musser would

not only be incapable of exchanging its endogenous quinone, it would not even be able to stabilise such a different range of semiquinones.

Another important conclusion that results from this work is that for the first time a 3 aromatic-ring inhibitor (anthraquinone) was successfully introduced inside a quinone binding site. A certain degree of specificity could be attached to this analogue, given its bulky structure, thus providing the basis of a different group of inhibitors not previously exploited.

High-field EPR scans that were run in order to obtain the g-values for each tensor proved to be very useful in determining the settings for future experiments. Metal composition greatly interfered in the resolution of the semiquinone spectra. Since hyperfine structures do not appear in high field experiments, it is likely that pursuing with these studies it will be possible to obtain the accurate g-tensors.

8.

References

8. References

Atherton , N M (1994) Principles of Electron Spin Resonance. Prentice Hall.

Babcock, G. T. and Wikstrom, M. (1992) *Nature* 356, 301-309.

Chepuri, V., Lemieux, L. J., Au, D. T.-C., and Gennis , R. B. (1990) *J. Biol. Chem.* 265, 11185-11192.

Ferguson-Miller, S., and Babcock, G. T. (1996) *Chem. Rev.* 96, 2889-2907.

Garcia-Horsman, J. A., Barquera, B., Rumbley, J., Ma, J., and Gennis, R. B. (1994) *J. Bacteriol.* 176, 5587-5600.

Gibson, Q. H. and Greenwood, C. (1963) *Biochem. J.* 86, 541-554

Glasnoe, P. K. & Long, L. A. (1960) *J. Phys. Chem.* 64, 188-190.

Hales, B. J. and Case, E. E. (1981) *Biochem. Biophys. Acta.* 637, 291-302.

Hallen, S., and Nilsson, T., (1992) *Biochemistry* 31, 11853-11859.

Hallen, S., Svensson, M., and Nilsson, T., (1993) *FEBS lett.* 325, 299-302.

Hastings, S. F. (1997) Studies of the Quinone Binding Sites of the *Escherichia coli* Terminal Oxidases, Cytochromes bo_3 & *bd*. PhD Thesis. University of St. Andrews. Scotland.

Hendler, R. W., Pardhasaradhi, K., Reynafarge, B., and Ludwig, B. (1991) *Biophys. J.* 60, 415-423.

Herweijer, M.A., Berden, J.A., Kemp, A., Slater, E.C. (1985) *Biochem. Biophys. Acta* 809, 81-89

Hoff, A.J., ed., (1989) Advanced EPR - Applications in Biology and Biochemistry, Elsevier

Ingledew, W. J., Ohnishi, T., Salerno, J. C. (1995) *Eur. J. Biochem.* 227, 903-908.

Kita, K., Konishi, K., and Anraku, Y. (1984) *J. Biol. Chem* 259, 3368-3374.

Kotlyar, A. B., Sled, V. D., Burdaev, D. S., Moroz, I. A. and Vinagradov, A. D. (1990) *FEBS Letts* 264, 17-20.

Ludwig, B., and Schatz, G. (1980) *Proc. Natl. Acad. Sci. U.S.A.* 77, 196-200.

Ma, J., Katsonouri, A., Gennis, R. B. (1997) *Biochemistry* 36, 11298-11303.

Ma, J., Lemieux, L. and Gennis, R. (1993) *Biochemistry* 32, 7692-7697.

MacMillan, F., Hanley, J., Van der Weerd, L., Knupling, M., Un, S. and Rutherford, A. W. (1997) *Biochemistry*, 36, 9297-9303.

Mitchell, P. (1976) *J. Theor. Biol.* 62, 327-367.

Mitchell, R., Moody, A. J. & Rich, P. R. (1995) *Biochemistry* 34, 7576-7585.

Mortan R. A (Ed.) (1965) *in* The Biochemistry of Quinones. Academic Press; London.

Murray, L., Pires, R., Ingledew, W.J. (1999) *Biochemical Society Transactions* 27, 581-585.

Musser, S.M., Stowell, M.H.B., Chan, S.I. (1993) *Febs Letters* 327, 131-136.

Musser, S. M., Stowell, M. H. B., Lee, H. K., Rumbley J. N. and Chan, S. I. (1997) *Biochemistry* 36, 894-902.

Orii, Y., Mogi, T., Sato-Watanabe, M., Hirano, T., and Anraku, Y. (1995) *Biochemistry* 34, 1127-1131.

Papa, S., Capitanio, N., Glasser, P. and Villani, G. (1994) *Cell Biol. Int.* 18, 345-355.

Poole, R. K. and Ingledew, W. J. (1987) in *Escherichia coli* and *Salmonella typhimurium* cellular and molecular biology (Neidhart, F. C., Ingraham, J. L., Low, K. B., Maganasaki, B., Schaechter, M. and Umbarger, E., eds) pp. 170-200, American Society for Microbiology. Washington, DC. USA.

Prochaska, L.J., Kirken, R.A., Hanrahan, G. and Lincoln, A.J. (1996) B*iophysical Journal* 70, 2, TUAM2

Puustinen, A., Morgan, J. E.,Verkhovsky, M., Thomas, J. W., Gennis, R. B., Wikström, M. (1992) *Biochemistry* 31, 10363-10369.

Puustinen, A., Verkhovsky, M. L., Morgan, J. E., Belevich, N. P. and Wikstrom, M. (1996) *Proc. Natl. Acad. Sci. U.S.A.* 93, 1545-1548.

Puustinen, A. and Wikström, M. (1991) *Proc. Natl. Acad. Sci. U.S.A.* 88, 6122-6128.

Saiki, K., Mogi., T., Ogura, K., and Anraku, Y. (1993) *J. Biol. Chem.* 268, 26041-26045.

Saiki, K., Nakamura, H., Mogi, T., Anraku, Y. (1996) *J. Biol. Chem.* 271, 26, 15336- 15340

Saraste, M. (1990) *Q. Rev. Biophys.* 23, 331-366.

Sato-Watanabe, M., Mogi, T., Takashi, O., Kitagawa, T., Miyoshi, H., Iwamura, H., Anraku, Y.(1994) *J. Biol. Chem.* 269, 28908-28912.

Sato-Watanabe, M, Itoh, S., Mogi, T., Matsuura, K., Miyoshi, H., Anraku, Y. (1995) *FEBS letters* 374, 265-269.

Sato-Watanabe, M., Mogi, T., Miyoshi, H., Anraku, Y. (1998) *Biochemistry* 37, 5356-5361.

Svensson-Ek, M. and Brzezinski, P. (1997) *Biochemistry* 36, 5425-5431.

Svensson-Ek, M., Thomas, J. W., Lemieux, L. J., Gennis, R. B., Nilsson, T. and Brzezinski, P. (1996) *Biochemistry* 35, 13673-13680.

Svensson, M., Hallen, S., Thomas, J. W., Lemieux, L.

Svensson, M., Hallen, S., Thomas, J. W., Lemieux, L. J., Gennis, R. B., and Nilsson, T. (1995) *Biochemistry* 34, 5252-5258.

Svensson, M.and Nilsson, T. (1993) *Biochemistry* 32, 5442-5447.

Trumpower, B. L., and Gennis, R. B. (1994) *Annu. Rev. Biochem.* 63, 675-716.

Villani, G., Tattoli, M., Capitanio, N., Glaser, P., Papa, S., and Danchin, A. (1995) *Biochem. Biophys. Acta* 1232, 67-74.

Warncke, A. B., Gunner, M. R., Braun, B. S., Gu, L., Yu, C.-A., Bruce, J. M. and Duton, P. L. (1994) *Biochemistry* 33, 7830-7841.

Weil, J A , Bolton , J R, Wertz , J E (1986) Electron Paramagnetic Resonance - Elementary Theory and Practical Applications , Wiley.

Welter, R., Gu, L-Q, Yu, L., Yu, C.-A., Rumbley, J. and Gennis, R. B. (1994) *J. Biol. Chem.* 269, 28834-28838.

Williams, R. J. P. (1961) *J. Theoret. Biol.* 1, 1-13.